Published in final edited form as:
J Cell Sci. 2008 May 15; 121(Pt 10): 1661–1670. doi:10.1242/jcs.020149.

PAI-1 stimulates fibronectin matrix assembly in osteosarcoma cells through crosstalk between the αvβ5 and α5β1 integrins

Daniel Vial and **Paula J. McKeown-Longo***
Center for Cell Biology and Cancer Research (MC-165) Albany Medical College 47 New Scotland Avenue Albany, New York 12208 USA

Summary

The plasminogen activation system regulates matrix remodeling through both proteolytic and non-proteolytic mechanisms. Studies were undertaken to determine the effects of the plasminogen activator inhibitor 1 (PAI-1) on fibronectin matrix assembly. The addition of PAI-1 to MG-63 cells caused a 1.5–3 fold increase in the rate of fibronectin matrix assembly which was associated with an increase in β1 integrin activation. PAI-1 treatment led to a marked decrease in focal contacts and stress fibers, while tensin-containing matrix contacts remained unaffected. The effects of PAI-1 on matrix assembly were independent of both uPA and uPAR, indicating that the stimulation of matrix assembly by PAI-1 did not depend on its anti-proteolytic activity or on the association of uPAR with integrin receptors. Antagonists of the αvβ5 integrin mimicked the effect of PAI-1 on cell morphology and fibronectin matrix deposition, indicating that stimulation of matrix assembly by PAI-1 required disruption of the interaction between the αvβ5 integrin and vitronectin. Consistent with this conclusion, the Q123K PAI-1 mutant which does not bind vitronectin had no effect on matrix assembly. Our data identify PAI-1 as a novel regulator of fibronectin matrix assembly and indicate that this regulation occurs through a previously undescribed crosstalk between the αvβ5 and α5β1 integrins.

Keywords

PAI-1; integrin; fibronectin; extracellular matrix; actin

Introduction

Fibronectin is widely expressed by multiple cell types and plays important roles in vertebrate development as well as in cell adhesion, migration, invasion, growth and differentiation. Formation of fibronectin matrix involves a cell-driven mechanical stretching of fibronectin, which is progressively incorporated into a dense detergent-insoluble fibrillar network via interactions with other cell-associated fibronectin dimers [reviewed in (Wierzbicka-Patynowski and Schwarzbauer, 2003)]. In most cell types, the α5β1 integrin is responsible for the polymerization of fibronectin matrix. The matrix assembly activity of the α5β1 integrin can be modulated by changes in the activation state of the integrin which occur in association with changes in integrin conformation (Mould et al., 2002). Changes in the level of activated α5β1 integrins on the cell surface can be induced by modifications in signaling pathways (Brenner et al., 2000) and through the formation of complexes with cytoskeletal components (Giannone et al., 2003). Cell surface molecules also regulate α5β1 integrin activation. Among them, uPAR, which is a GPI-anchored molecule has been reported to form physical complexes

*Author for Correspondence: Center for Cell Biology & Cancer Research, Mail Code 165, Albany Medical College, 47 New Scotland Ave, Albany, NY 12208, Telephone: 518-262-5651, Fax: 518-262-5669, E-mail: mckeowp@mail.amc.edu.

with integrins, including α5β1 and modulate their function (Aguirre-Ghiso et al., 2001; Wei et al., 1996). More recently, we have shown that uPAR can increase fibronectin matrix deposition and α5β1 integrin activation through a Src/EGFR signaling pathway which does not depend on the formation of uPAR/α5β1 complexes (Monaghan-Benson and McKeown-Longo, 2006).

The plasminogen activator system is involved in matrix remodeling through regulation of uPA activity, which converts plasminogen into plasmin and thus mediates pericellular proteolysis [for review see (Schmitt et al., 1992)]. Plasminogen activator inhibitor Type I (PAI-1) is the main in vivo inhibitor of uPA, thus playing a role in extracellular matrix turnover by regulating pericellular plasmin. In addition to plasmin mediated remodeling, the plasminogen activator system also modulates cell behavior through non-proteolytic events. Both PAI-1 and uPAR bind to the adhesive protein vitronectin. Vitronectin binds PAI-1 with high affinity and regulates PAI-1 activity by stabilizing PAI-1 in its active conformation. The PAI-1 binding site on vitronectin lies in the amino-terminal SMB domain and functionally overlaps with both the uPAR and integrin binding sites. PAI-1 is able to competitively inhibit the binding of uPAR and integrin to vitronectin and has been reported to both stimulate and inhibit cell migration (Deng et al., 2001; Okumura et al., 2002; Stefansson and Lawrence, 1996). On the other hand, PAI-1 can also regulate integrin function through another mechanism which does not require its interaction with vitronectin. PAI-1 has been shown to deactivate integrins by binding to the uPA present in uPA-uPAR-integrin complexes on the cell surface resulting in the inactivation of the integrin and the subsequent detachment of cells from the matrix. This activity of PAI requires the binding of PAI to uPAR bound uPA (Czekay et al., 2003).

We have shown previously that PAI-1 can work synergistically with a uPAR agonist to stimulate fibronectin matrix assembly in human osteosarcoma cells (Vial et al., 2006). The current study was undertaken to examine the mechanism underlying the stimulation of fibronectin matrix assembly by PAI-1. Earlier reports have shown that vitronectin inhibits the assembly of the fibronectin matrix (Hocking et al., 1999; Zhang et al., 1999) and that this inhibition depends on the binding of vitronectin integrins to vitronectin (Zheng et al., 2007). We, therefore, hypothesized that PAI-1 might stimulate matrix assembly by relieving the inhibitory effects of vitronectin. We now report that PAI-1 causes an increase in fibronectin matrix assembly and in the activation of the α5β1 integrin. The effect of PAI-1 on matrix assembly was uPAR and uPA independent and resulted from an inhibition of the interaction between the αvβ5 integrin and vitronectin. These findings indicate that the regulation of matrix assembly by PAI occurs through a novel pathway of crosstalk between the αvβ/5 and α5β1 integrin receptors.

RESULTS

PAI-1 increases fibronectin matrix assembly through a uPA/uPAR-independent mechanism

Incubation of MG-63 cell monolayers with PAI-1 resulted in a dose-dependent increase in fibronectin matrix assembly (Fig. 1). Stimulation of matrix assembly was seen at 5 nM PAI-1 and maximal levels of fibronectin deposition were observed at 100 nM PAI-1. Increasing the amount of PAI-1 beyond 100 nM resulted in no further stimulation (data not shown). To test whether the binding of PAI-1 to either vitronectin or uPA was required for the stimulatory effect of PAI-1 on matrix formation, MG-63 cells were incubated with mutant forms of PAI-1 deficient in specific binding activities. The Q123K mutant which does not bind to vitronectin had no effect on fibronectin matrix assembly, indicating that the binding of PAI-1 to vitronectin was required to increase assembly of fibronectin matrix. This result was in agreement with our earlier experiments using cells adherent to either vitronectin or fibronectin substrates, where PAI-1 (under conditions of uPAR stimulation) caused an increase in matrix assembly only in the presence of vitronectin (Vial et al., 2006). The PAI-1R mutant, which does not bind to uPA

but does bind to vitronectin, increased fibronectin polymerization to the same extent as wild-type PAI-1, suggesting that the stimulatory effects of PAI-1 on matrix assembly requires binding to vitronectin, but does not require the association of PAI-1 with uPA. Fig. 1B shows that treatment of cells with PAI-1 caused a small, but significant increase in the number of activated β1 integrins. There was no change in the total amount of β1 integrin (data not shown). As reported previously (Vial et al., 2006), ligation of uPAR with the peptide agonist, P25, also increased integrin activation and this activation was further enhanced by PAI-1.

PAI-1 binds vitronectin in close proximity to the uPAR binding site and can competitively inhibit the binding of uPAR to vitronectin (Deng et al., 1996). To evaluate the role of uPAR on the PAI-1 stimulation of matrix assembly, uPAR was knocked down in MG-63 cells using siRNA. Fig. 2A indicates that uPAR expression was almost completely inhibited in MG-63 cells transfected with uPAR siRNA. uPAR knockdown had no effect on the expression of actin or on the expression of the β5 integrin. Treatment of uPAR knockdown cells with PAI-1 stimulated matrix assembly to levels seen in control cells (Fig. 2B). In contrast, stimulation of matrix assembly by the uPAR ligand, P25, was severely attenuated in uPAR knockdown cells (Fig. 2C). Taken together with the results in Fig. 1, these data demonstrate that the PAI-1 dependent stimulation of integrin activation and matrix assembly depend on the binding of PAI-1 to vitronectin but do not require either uPA or uPAR.

Disruption of the αvβ5-vitronectin interaction increases fibronectin matrix assembly

Our results indicate that the binding of PAI-1 to vitronectin increases fibronectin matrix deposition by MG-63 cells. The PAI-1 binding site on vitronectin is close to the RGD motif of vitronectin and PAI-1 binding can sterically inhibit integrin dependent adhesion to this motif (Lawrence et al., 1994). To determine whether the PAI-1 mediated effects on matrix assembly resulted from a loss of vitronectin receptor binding to vitronectin, cells were incubated with blocking antibodies and peptides to disrupt the association of integrin receptors with vitronectin. Treatment of MG-63 cells with the cyclic peptide RGDfV, which disrupts the interaction of αvβ3 and αvβ5 integrins with vitronectin, led to an increase in fibronectin matrix deposition (Fig. 3A). No effect was observed when the inactive analog RADfV was used. Control adhesion and spreading experiments indicated that the RGDfV peptide completely blocked adhesion of cells to vitronectin but had no effect on adhesion or spreading of cells on fibronectin (data not shown). Incubation of cells with the αvβ3 integrin blocking antibody, LM609, had no effect on fibronectin assembly. However, treatment of cells with the β5 integrin blocking antibody, P1F6, significantly increased fibronectin matrix assembly (Fig. 3A).

Our previous studies have shown that treatment of MG-63 cells with the uPAR agonist, P25, caused a several-fold increase in the rate of matrix assembly and that the addition of PAI-1 caused a further increase in matrix assembly. To determine whether the effects of integrin antagonists on matrix assembly occur under conditions of uPAR stimulation, cells were incubated with P25 in the presence of vitronectin receptor antagonists, RGDfV or P1F6. Incubation of cells with P25 resulted in a 9-fold increase in fibronectin matrix assembly. This rate of matrix assembly was further increased to nearly 15-fold above baseline in the presence of peptide antagonists of the vitronectin receptor (Fig. 3B). Similar results were seen when cells were incubated with the αvβ5 blocking antibody, P1F6. These data indicate that the effects of PAI-1 on matrix assembly can be mimicked by agents which disrupt αvβ5 binding to vitronectin. Similar effects of PAI-1 and integrin disrupting agents were seen in three other cell lines. As shown in Fig. 4A, treatment of human osteosarcoma cells (HOS, Saos-2) or osteoblasts (hFOB) with either PAI-1 or RGDfV caused a 30–50% increase in fibronectin matrix assembly. PAI-1 and RGDfV also increased matrix assembly by several fold when added to the cells under conditions of uPAR stimulation (Fig. 4B).

Disruption of αvβ5-vitronectin interaction leads to an increase in β1 integrin activation

As shown in Fig. 1B, the addition of PAI-1 to MG-63 cells caused a significant increase in activated β1 integrin on the cell surface. To determine whether antagonists of the αvβ5 integrin can modulate α5β1 integrin activation, ELISA assays were performed. Cells were treated with either the cyclic peptide RGDfV or with the integrin αvβ5 blocking antibody (PIF6) and the amount of activated β1 integrin was assessed using antibodies which recognize the active conformer (Fig. 5). The RGDfV peptide (A) and the PIF6 antibody (B) increased β1 activation under basal conditions and under conditions of uPAR stimulation with P25. β1 integrin activation was increased to levels similar to that seen with PAI-1 (compare with Fig. 1B). There was no change in total β1 integrin (data not shown). The control peptide RADfV and mouse IgG had no effect on β1 integrin activation. These data suggest that the disruption of the αvβ5 integrin-vitronectin interaction leads to an increase in both β1 integrin activation and fibronectin matrix assembly.

PAI-1 disrupts αvβ5-containing adhesions and actin stress fibers

To evaluate whether the addition of exogenous PAI-1 to cells was disrupting the binding of αvβ5 to vitronectin, αvβ5 receptor localization was visualized by indirect immunofluorescence. As shown in Fig. 6, control cells express numerous clusters of αvβ5, which are co-localized with paxillin in focal contacts (panels a, e, i). Treatment of cells with PAI-1 lead to a marked decrease in the number of focal contacts with fewer clusters of β5 integrins and decreased paxillin staining (panels b, f, j). Similar results were seen when cells were treated with the PAI-1 mutant, PAI-1R, which binds to vitronectin but does not bind to uPA (panels c, g, k). Treatment of cells with the PAI-1 mutant (Q123K), which does not bind vitronectin, failed to disrupt the focal contacts (panels d, h, l). These data have been quantified in Table 1 to show that over 90% of the cells exhibit marked decreases in focal contact numbers. The PAI-1 mediated disruption of focal contacts was also associated with a change in the organization of actin filaments. As shown in Fig. 7, cells treated with PAI-1 exhibited a loss of stress fibers associated with the appearance of actin aggregates at the periphery of the cell (compare panels a, b). The PAI-1R mutant also disrupted actin filament structure (panel c) indicating that the effect of PAI-1 on stress fibers did not require uPA binding. The PAI-1 Q123K mutant had no effect on actin organization (panel d) consistent with a requirement for vitronectin binding in the effect of PAI-1 on cytoskeletal organization. The PAI-1 induced loss of stress fibers was accompanied by fewer clusters of β5 integrin receptors (panels e-h). These data indicate that the addition of PAI-1 to MG-63 cells results in the loss of both focal contacts and actin stress fibers and that this activity requires the binding of PAI-1 to vitronectin.

uPAR also binds to vitronectin and is present within the αvβ5-vitronectin contacts [(Fig. 8A, panels a-c; see also (Salasznyk et al., 2007)]. To evaluate whether uPAR was required for the PAI-1 induced disruption of αvβ5-vitronectin contacts, PAI-1 was added to cells in which uPAR had been knocked down. Treatment of cells with uPAR siRNA (see also Fig. 2A) results in a complete loss of uPAR staining in focal contacts (Fig. 8B, panels a and d) with no loss of paxillin staining (Fig. 8B, panels b and e), indicating that uPAR knockdown does not affect the localization of paxillin to focal adhesions. uPAR knockdown also had no effect on β5 integrin clustering (Fig. 8C, panel b) indicating that it did not affect the binding of the αvβ5 integrin to vitronectin. Incubation of uPAR knock-down cells with PAI-1 shows nearly complete loss of clustered β5 integrin (Fig. 8C, panel d). These data suggest that the disruption of αvβ5 binding to vitronectin by PAI-1 is independent of uPAR.

PAI-1 does not affect matrix adhesion—Although treatment of MG-63 cells with PAI-1 disrupted the association of αvβ5 with vitronectin, there was no cell detachment. As shown in Fig. 9A (Panel a), MG-63 cells assembled a fibronectin matrix and this matrix was still present on PAI-1 treated cells under conditions where β5 clustering was disrupted (Fig. 9A, panels c

and d). Furthermore, Fig. 9B shows the co-localization of fibronectin with activated β1 integrins (panels a–c). This co-localization was still present after PAI-1 treatment (panels d-f), suggesting that PAI-1 treatment does not disrupt fibronectin-based matrix adhesions. To evaluate this possibility further, cells were stained for tensin as a marker for matrix adhesions. As shown in Fig. 10A, MG-63 cells exhibited prominent staining for tensin which co-distributed extensively with matrix fibronectin, indicating the presence of matrix adhesions on these cells. These adhesions were present after treatment of cells with PAI-1. Figure 10B shows that control cells have both paxillin and tensin containing adhesions. The merged figure shows little co-localization of these adhesions indicating that they represent distinct structures. Treatment of cells with PAI-1 caused a nearly complete loss of paxillin staining while considerable tensin staining remained (Fig. 10B). These data indicate that the addition of PAI to cells disrupts αvβ5/paxillin-containing focal contacts while α5β1/tensin containing matrix adhesions are maintained.

β5 knockdown attenuates PAI-1 mediated increases in matrix assembly—To confirm the role of the αvβ5 integrin in the PAI-1 stimulation of matrix assembly, the β5 integrin subunit was knocked down in MG-63 cells using β5 integrin siRNA. Fig. 11A indicates that knockdown of the β5 integrin subunit decreased expression of β5 protein. Scanning of Western blots from cell lysates showed that the extent of knockdown was 50% (data not shown). β5 knockdown resulted in a 50% increase in basal (control) levels of matrix assembly (Fig. 11B). The addition of PAI-1 to cells transfected with control siRNA resulted in a 2-fold increase in fibronectin matrix assembly. However, matrix assembly in cells transfected with β5 siRNA was stimulated only 25% following PAI-1 addition (Fig. 11C). Taken together our data suggest that PAI-1 increases fibronectin matrix deposition by inhibiting the interaction between αvβ5 integrin and vitronectin and provide evidence for a previously unrecognized crosstalk between the αvβ5 and α5β1 integrins.

Discussion

Our earlier studies have demonstrated that the assembly of the fibronectin matrix is under complex regulation by the plasminogen activator system. PAI-1 and uPAR have been shown to synergistically stimulate fibronectin polymerization (Monaghan et al., 2004; Monaghan-Benson and McKeown-Longo, 2006; Vial et al., 2006). In the current study, we show that PAI-1 stimulates matrix assembly by activating a previously undescribed crosstalk between the αvβ5 and α5β1 integrins. PAI-1 stimulation of matrix assembly occurred over the range of 5–100 nM. Earlier studies have shown that the binding of PAI-1 to vitronectin occurs at nM concentrations (Seiffert and Loskutoff, 1991), and that PAI-1 is present in the subcellular matrix at nM levels (Higgins et al., 1989). These data indicate that the effects of PAI-1 on matrix assembly are seen at physiologically relevant concentrations. The effects of PAI-1 on matrix assembly are dependent on vitronectin, but do not require uPAR. The stimulation of matrix assembly by PAI-1 is relatively modest (1.5–2.5 fold) but is similar to previously reported effects of PAI-1 on the stimulation of cell migration (Degryse et al., 2005; Isogai et al., 2001; Takahashi et al., 2005).

The disruption of focal contacts by PAI-1 can be mimicked by antagonists of the αvβ5 integrin, suggesting that PAI-1 is displacing the integrin from vitronectin. The PAI-1 binding site on vitronectin functionally overlaps with the integrin binding site, however, it is unlikely that PAI is actively displacing previously bound integrin. More likely, PAI-1 is binding to vitronectin when a binding site becomes open secondary to vitronectin receptor trafficking out of the focal contact. Studies indicate that active remodeling of contacts occurs and that the expected half-life of a focal contact can be as short as a few minutes (Edlund et al., 2001; Franco et al., 2006). Vitronectin has been shown to negatively regulate matrix assembly (Hocking et al., 1999; Zhang et al., 1999) through a mechanism requiring vitronectin integrin receptors (Zheng

et al., 2007). This suggests that PAI-1 is relieving an inhibitory activity of the αvβ5 integrin. The loss of vitronectin receptor binding results in a loss of actin stress fibers and a decrease in paxillin-containing focal adhesions. PAI-1 treatment had no effect on matrix adhesions as tensin and α5β1 remained co-localized with fibronectin matrix. These data indicate that the effects of PAI-1 on cell adhesion are selective, causing a loss of focal adhesions but having no effect on matrix adhesions. The data also indicate that β1 integrin activation occurs in the absence of stress fibers and that focal contacts, but not matrix adhesions, support stress fiber organization in these cells. These findings are consistent with earlier reports in HT-1080 cells showing that actin stress fibers are not required for fibronectin matrix assembly (Brenner et al., 2000). Our data suggest that the disengagement of αvβ5 integrin from vitronectin stimulates fibronectin matrix assembly by increasing the number of activated α5β1 integrins on the cell surface. The mechanism by which the disruption of the αvβ5-vitronectin interaction by PAI-1 regulates α5β1 integrin function is unclear. The disengagement of αvβ5 integrins results in organizational changes in actin which may impact the association of the α5β1 integrin with cytoskeleton-associated proteins involved in integrin activation [reviewed in (Arnaout et al., 2007)].

Our earlier studies have shown that uPAR agonists can stimulate matrix assembly through inside-out signaling pathways leading to integrin activation (Monaghan-Benson and McKeown-Longo, 2006). PAI-1 can further stimulate matrix assembly under conditions of uPAR ligation resulting in synergistic increases in matrix assembly rates (Vial et al., 2006). In the present study, we show that treatment of cells with PAI-1 stimulates matrix assembly and integrin activation under conditions of uPAR knockdown. These results suggest that PAI and uPAR regulate matrix assembly through independent pathways, which converge at the level of integrin activation. Previous studies have shown that the addition of PAI-1 to HT-1080 cells causes inactivation of both β3 and β1 integrins (Czekay et al., 2003). In these studies, integrin inactivation by PAI-1 required the binding of PAI-1 to uPAR bound uPA. However, in our studies PAI-1 could disrupt the association of αvβ5 integrin with vitronectin, but we found no requirement for uPA or uPAR in the PAI-1 mediated loss of αvβ5 containing adhesions. We also found that PAI-1 strengthened rather than disrupted the association of β1 with the fibronectin matrix. The basis for this discrepancy is not clear but may have to do with the amounts of PAI-1 used in each of the studies. PAI-1-mediated integrin inactivation required 40-fold higher levels of PAI-1 (800 nM) than the amounts used in our studies where disruption of focal contacts and stimulation of matrix assembly were seen at 20 nM PAI-1.

A recent study has shown that cells adhering to vitronectin in the presence of PAI-1 are only partially inhibited from attachment (Stefansson et al., 2007). The cells which can overcome the inhibitory effects of PAI-1 on adhesion are partially spread and do not assemble either focal contacts or stress fibers. Adhesion of these cells to vitronectin in the presence of PAI-1 required polymerized microtubules and actin. Our results are consistent with these findings and extend them to show that the addition of PAI-1 to adherent monolayers of osteosarcoma cells causes a fairly rapid (<3 hours) disruption of previously formed focal contacts and stress fibers. Taken together, these results suggest that cells can modulate the effects of PAI-1 on cell adhesion or matrix assembly by altering the association of vitronectin integrin receptors with the cytoskeleton.

Increased PAI-1 levels are seen in many cancers and are positively correlated with disease progression (Chambers et al., 1998; Foekens et al., 2000). The balance between local PAI-1 concentrations and integrin activation may have important implications for processes such as angiogenesis and/or tumor cell metastasis where leaky blood vessels would contribute to increased amounts of vitronectin in the matrix. Previous studies using haptotaxis assays have shown that preincubation of vitronectin with PAI-1 blocks cell binding to vitronectin and promotes migration of cells toward fibronectin (Isogai et al., 2001). Our studies show that the

incubation of adherent cells with PAI-1 stimulates the activation of the α5β1 integrin and increases the rate of fibronectin polymerization. The effects of PAI-1 on matrix assembly and cell motility are both dependent on vitronectin and suggest that the two PAI-1 dependent phenomena may function in concert to support directed cell migration by coupling the recycling of vitronectin receptors to the polymerization of the fibronectin matrix.

Materials and Methods

Reagents and Antibodies

Unless otherwise stated, all chemicals were purchased from Sigma (St. Louis, MO). The uPAR ligand, peptide P25, sequence AESTYHHLSLGYMYTLN, and the scrambled peptide, S25, sequence NYHYLESSMTALYTLGH, were synthesized by Cell Essentials (Boston, MA). uPAR siRNA sequence (GGTGAAGAAGGGCGTCCAA), β5 integrin siRNA (GAACAACGGTGGAGATTTT) and non-targeting control siRNA pool were purchased from Dharmacon. The RGDfV peptide, selective for vitronectin integrins, and the inactive analog RADfV were purchased from Sigma. The selectivity of this peptide was verified in control experiments which showed that RGDfV had no effect on α5β1 function. The anti-β_1 antibodies, clones P5D2 and HUTS-4 were purchased from Chemicon (Temecula, CA). The 9EG7, tensin and FITC labeled paxillin antibodies were obtained from Pharmingen (San Diego, CA). The β5 integrin antibody clones P1F6 and 15F11 (used for the immunofluorescence experiments) were from Chemicon (Temecula, CA). The rabbit β5 integrin antibody (used for Western Blot) was from Abcam (Cambridge, England). Control mouse IgG and antibody to β-actin were obtained from Sigma (St. Louis, MO). Secondary antibodies goat anti-mouse and goat anti-rabbit HRP were purchased from Bio-Rad (Hercules, CA). AlexaFluor^{594}-labeled goat anti-rat antibody was obtained from Molecular Probes (Eugene, OR). Recombinant active PAI-1 and the non-vitronectin binding PAI-1 mutant, Q123K, were from Molecular Innovations (Southfield, MI). The dual mutant PAI-1R (T333→R and A335→R) which does not bind uPA was kindly provided by Dr. D. Lawrence (Internal Medicine, University of Michigan Medical School, Ann Arbor, MI). The uPAR polyclonal antibody was a kind gift from Dr Andrew Mazar (Attenuon, San Diego, CA).

Cell Culture

The MG-63 and HOS human osteosarcoma cells were obtained from ATCC and maintained in Dulbecco's modified Eagle's medium (DMEM, Invitrogen), containing antibiotics (penicillin-streptomycin) and 10% fetal bovine serum (FBS, Hyclone Laboratories, Logan, UT). Saos-2 human osteosarcoma cells were from ATCC and were cultured in DMEM containing 15% FBS. Human fetal osteoblasts (HFOB) cells were obtained from ATCC and were cultured in DMEM/F12 media without phenol red containing 10% FBS, as described previously (Harris et al., 1995).

siRNA experiments

For the β5 knockdown, electroporation was performed using the SIPORT electroporation buffer from Ambion. In each electroporation cuvette (Genesee Scientific, San Diego, CA), 1.5 μg of siRNA was added to 9×10^4 cells, and the electroporation was performed at 450 volts, 4 Pulses 100 μs, separation between pulses 100 ms. Cells were then cultured in 6-well plates for 4 days in complete medium. For the uPAR siRNA experiments, cells were transfected as above and then retransfected on day 2 using Dharmafect 2 as recommended by the manufacturer (Dharmacon). Twenty-four hours later, uPAR knockdown cells were replated and experiments were performed the following day.

Purification of Fibronectin and Vitronectin

Human plasma fibronectin was purified from a fibronectin- and fibrinogen-rich by-product of Factor VIII production by ion exchange chromatography on DEAE-cellulose (Amersham Biosciences) and iodinated as described previously (Zheng and McKeown-Longo, 2002). Vitronectin was purified from fibronectin- and fibrinogen-depleted human plasma by heparin-Sepharose affinity chromatography according to the method of Yatohgo et al. (1988). Iodinated fibronectin was mixed with bovine albumin, 1 mg/ml, dialyzed against phosphate-buffered saline, and frozen at −80°C until used. Fibronectin (2 mg/ml) was derivatized with AlexaFluor^{488} according to the manufacturer's protocol (Molecular Probes).

Matrix Incorporation Assay

Cells were seeded onto 6 well plates (2.2×10^5 cells/well) in complete medium. The following day, cultures were incubated for 6 hours with ^{125}I-fibronectin (2 μg/ml; 1×10^6 cpm/ml) in DMEM +0.02% BSA + 20 mM Hepes in the presence or the absence of PAI-1, PAI-1 mutants or various peptides or antibodies as described in the figure legends. For isolation of detergent insoluble matrix, cells were rinsed in PBS, extracted in 1% deoxycholate (DOC) (in 20 mM Tris pH 8.8) buffer containing 2 mM phenylmethylsulfonyl fluoride, 2 mM EDTA, 2 mM N-ethylmaleimide, and 2 mM iodoacetic acid). Detergent insoluble matrix was obtained by centrifugation at 18,000 rpm for 40 minutes and associated radioactivity present in the pellet measured using gamma scintillation. To determine the total cell layer-associated fibronectin, cells were rinsed 3 times in PBS, scraped directly into 1 ml of 1% deoxycholate and the total cell layer associated ^{125}I-fibronectin was determined by gamma scintillation.

Fluorescent Microscopy

MG-63 cells were cultured overnight (30×10^3 cells/coverslip) in DMEM containing 10% serum. Cell were washed and incubated for 3 hours in DMEM+BSA 0.02% + 20 mM Hepes in the absence or presence of 20 nM PAI-1 (or PAI-1 mutants), RGDfV or its inactive analog RADfV (20 μM). Cells were rinsed, fixed with 3% paraformaldehyde, permeabilized with 0.5% Triton for 10 minutes and blocked for 1 hour with 3% BSA in PBS. Coverslips were incubated in PBS+1% BSA with the primary antibody as described in the figure legends. Cells were washed in PBS for 5 minutes and incubated with AlexaFluor^{488}-or AlexaFluor^{594}-labeled secondary antibody. After staining, the coverslips were mounted with Prolong Antifade according to manufacturer's instructions (Molecular Probes, Eugene, OR). Slides were examined using an Olympus BMX-60 microscope equipped with a cooled CCD sensi-camera (Cooke, Auburn Hills, MI). Images were acquired using Slidebook software (Intelligent Imaging Innovation, Denver, CO) and processed with Photoshop program (Adobe).

Cell lysis and immunoblot analysis

Cell layers were washed with PBS before solubilization in cell-lysis buffer containing 20 mM Tris-HCl, pH 7.4, 1% Triton X-100, 0.5% NP-40, 0.15 M NaCl, 1 mM Na_3VO_4, and one mini-tablet of complete-protease-inhibitor per 10 ml (Roche, Indianapolis, IN). After incubation on ice for 30 minutes, cell lysates were centrifuged at 20,800 g for 15 minutes at 4°C and the insoluble pellets were discarded. The protein concentration of the lysate was determined using a BCA protein assay reagent (Pierce, Rockford, IL). Aliquots of cell lysates containing equal amounts of protein were subjected to SDS-PAGE on a 8% polyacrylamide gel under non-reducing conditions, followed by transfer to nitrocellulose membrane. Proteins were detected by western blot with a chemiluminescence reagent (Amersham Biosciences, Piscataway, NJ).

Integrin Activation Assay

Activation of the β1 integrin was assessed by ELISA using either the HUTS-4 or the 9EG7 antibody as described previously (Monaghan et al., 2004). These antibodies recognize the

activated conformation of the β1 integrin. Total β1 integrin was measured using the P5D2 antibody that recognizes all forms of β1 integrin. Cells were incubated with antibodies (100 ng/ml) for 1 hour at 37°C, rinsed with PBS and fixed with 3% paraformaldehyde. Following blocking with 3% BSA, cells were incubated for 1 hour with HRP-conjugated goat anti-mouse antibody. Freshly prepared substrate (0.1 M citrate buffer, 0.5 mg/ml *o*-phenylenediamine, 1 μl/ml 30% hydrogen peroxide pH 5.0) was added to each well, and the color was allowed to develop. The reaction was stopped with the addition of 2 N sulfuric acid, and the OD was measured at A^{490}. Measurements were corrected for light scattering by subtracting the OD obtained at A^{650}.

Acknowledgements

These studies were supported by Grant CA-58626 from the National Institutes of Health (NIH) (to P. M.-L.). The authors thank Drs. Dan Lawrence and R.P. Czekay for their generous gift of reagents.

References

Aguirre-Ghiso JA, Liu D, Mignatti A, Kovalski K, Ossowski L. Urokinase receptor and fibronectin regulate the ERK(MAPK) to p38(MAPK) activity ratios that determine carcinoma cell proliferation or dormancy in vivo. Mol Biol Cell 2001;12:863–879. [PubMed: 11294892]

Arnaout MA, Goodman SL, Xiong J. Structure and mechanics of integrin-based cell adhesion. Current Opin Cell Biol 2007;19:495–507.

Brenner KA, Corbett SA, Schwarzbauer J. Regulation of fibronectin matrix assembly by activated Ras in transformed cells. Oncogene 2000;19:3156–3163. [PubMed: 10918570]

Chambers SK, Irvins CM, Carcamgiu ML. Plasminogen activator inhibitor-1 is an independent poor prognostic factor for survival in advanced stage epithelial ovarian cancer patients. Int J Cancer 1998;79:449–454. [PubMed: 9761111]

Czekay RP, Aertgeerts K, Curriden SA, Loskutoff D. Plasminogen activator inhibitor-1 detaches cells from extracellular matrices by inactivating integrins. J Cell Biol 2003;160:781–791. [PubMed: 12615913]

Degryse B, Resnati M, Czekay RP, Loskutoff DJ, Blasi F. Domain 2 of the urokinase receptor contains an integrin-interacting epitope with intrinsic signaling activity: Generation of a new integrin inhibitor. J Biol Chem 2005;280:24792–24803. [PubMed: 15863511]

Deng G, Curriden SA, Hu G, Czekay RP, Loskutoff DJ. Plasminogen activator inhibitor-1 regulates cell adhesion by binding to the somatomedin B domain of vitronectin. J Cell Physiol 2001;189:23–33. [PubMed: 11573201]

Deng G, Curriden SA, Wang S, Rosenberg S, Loskutoff DJ. Is plasminogen activator inhibitor-1 the molecular switch that governs urokinase receptor-mediated cell adhesion and release? J Cell Biol 1996;134:1563–1571. [PubMed: 8830783]

Edlund M, Lotano MA, Otey CA. Dynamics of a-actinin in focal adhesion and stress fibers visualized with a-actinin-green fluorescent protein. Cell Motil Cytoskeleton 2001;48:190–200. [PubMed: 11223950]

Foekens JA, Peters HA, Look MP, Po9rtengen H, Schmitt M, Kramer MD, Brunner N, Janicke F, Meijer-van Gelder ME, Henzen-Logmans SC, van Putten WL, Klign JG. The urokinase system of plasminogen activation and prognosis in 2780 breast cancer patients. Cancer Res 2000;60:636–643. [PubMed: 10676647]

Franco P, Vocca I, Carriero MV, Alfano D, Cito L, Longanesi-Cattani I, Grieco P, Ossowski L, Stoppelli MP. Activation of urokinase receptor by a novel interaction between the connecting peptide region of urokinase and αvβ5 integrin. J Cell Sci 2006;119:3424–3434. [PubMed: 16882693]

Giannone G, Jiang G, Sutton DH, Critchley DR, Sheetz MP. Talin1 is critical for force-dependent reinforcement of initial integrin-cytoskeleton bonds but not tyrosine kinase activation. J Cell Biol 2003;163:409–419. [PubMed: 14581461]

Harris S, Enger RJ, Riggs BL, Spelsberg TC. Development and characterization of a conditionally immortalized human fetal osteoblastic cell line. J Bone Miner Res 1995;10:178–186. [PubMed: 7754797]

Higgins PJ, Ryan MP, Chaudhari P. Cytochalasin D-mediated hyperinduction of the substrate-associated 52-kilodalton protein p52 in rat kidney fibroblasts. J Cell Physiol 1989;139:407–417. [PubMed: 2715193]

Hocking DC, Sottile J, Reho T, Fassler R, McKeown-Longo PJ. Inhibition of fibronectin matrix assembly by the heparin-binding domain of vitronectin. J Biol Chem 1999;274:27257–27264. [PubMed: 10480945]

Isogai C, Laug WE, Shimada H, Declerck PJ, Stins MF, Durden DL, Erdreich-Epstein A, DeClerck YA. Plasminogen activator inhibitor-1 promotes angiogenesis by stimulating endothelial cell migration toward fibronectin. Cancer Res 2001;61:5587–5594. [PubMed: 11454712]

Lawrence DA, Berkenpas MB, Palaniappan S, Ginsburg D. Localization of vitronectin binding domain in plasminogen activator inhibitor-1. J Biol Chem 1994;269:15223–15228. [PubMed: 7515053]

Monaghan E, Gueorguiev V, Wilkins-Port C, McKeown-Longo PJ. The receptor for urokinase-type plasminogen activator regulates fibronectin matrix assembly in human skin fibroblasts. J Biol Chem 2004;279:1400–1407. [PubMed: 14602715]

Monaghan-Benson E, McKeown-Longo PJ. uPAR regulates a novel pathway of fibronectin matrix assembly requiring Src dependent transactivation of EGFR. J Biol Chem 2006;281:9450–9459. [PubMed: 16461772]

Mould AP, Askari JA, Barton S, Kline AD, McEwan PA, Craig SE, Humphries MJ. Integrin activation involves a conformational change in the α1 helix of the β subunit A-domain. J Biol Chem 2002;277:19800–19805. [PubMed: 11893752]

Okumura Y, Kamikubo Y, Curriden SA, Wang J, Kiwada T, Futaki S, Kitagawa K, Loskutoff DJ. Kinetic analysis of the interaction between vitronectin and the urokinase receptor. J Biol Chem 2002;277:9395–9404. [PubMed: 11773078]

Salasznyk RM, Zappala M, Zheng M, Yu L, Wilkins-Port C, McKeown-Longo PJ. The uPA receptor and the somatomedin B region of vitronectin direct the localization of uPA to focal adhesions in microvessel endothelial cells. Matrix Biol 2007;26:359–370. [PubMed: 17344041]

Schmitt M, Janicke F, Moniwa N, Chucholowski N, Pache L, Graeff H. Tumor-associated urokinase type plasminogen activator: biological and clinical significance. Biol Chem Hoppe Seyler 1992;373:611–622. [PubMed: 1515091]

Seiffert D, Loskutoff DJ. Kinetic analysis of the interaction between type 1 plasminogen activator inhibitor and vitronectin and evidence that the bovine inhibitor binds to a thrombin-derived amino-terminal fragment of bovine vitronectin. Biochim Biophys Acta 1991;1078:23–30. [PubMed: 1710930]

Stefansson S, Lawrence DA. The serpin PAI-1 inhibits cell migration by blocking integrin $\alpha_v\beta_3$ binding to vitronectin. Nature 1996;383:441–443. [PubMed: 8837777]

Stefansson S, Su EJ, Ishigami S, Cale JM, Gao Y, Gorlatova N, Lawrence DA. The contributions of integrin affinity and integrin-cytoskeletal engagement in endothelial and smooth muscle cell adhesion to vitronectin. J Biol Chem 2007;282:15679–15689. [PubMed: 17403662]

Takahashi T, Suzuki K, Ihara H, Mogami H, Kazui T, Urano T. Plasminogen activator inhibitor type 1 promotes fibrosarcoma cell migration by modifying cellular attachment to vitronectin via αvβ5 integrin. Semin Thromb Hemost 2005;31:356–363. [PubMed: 16052409]

Vial D, Monaghan-Benson E, McKeown-Longo PJ. Coordinate regulation of fibronectin matrix assembly by the plasminogen activator system and vitronectin in human osteosarcoma cells. Cancer Cell Intl 2006;6:8.

Wei Y, Lukashev M, Simon DI, Bodary SC, Rosenberg S, Doyle MV, Chapman HA. Regulation of integrin function by the urokinase receptor. Science 1996;273:1551–1555. [PubMed: 8703217]

Wierzbicka-Patynowski I, Schwarzbauer JE. The ins and outs of fibronectin matrix assembly. J Cell Sci 2003;116:3269–3276. [PubMed: 12857786]

Yatohgo T, Izumi M, Kashiwagi H, Hayashi M. Novel purification of vitronectin from human plasma by heparin affinity chromatography. Cell Struct Funct 1988;13:281–292. [PubMed: 2460263]

Zhang Q, Peyruchaud O, French KJ, Magnusson MK, Mosher DF. Sphingosine 1-phosphate stimulates fibronectin matrix assembly through a Rho-dependent signal pathway. Blood 1999;93:2984–2990. [PubMed: 10216094]

Zheng M, Ambesi A, Yu L, McKeown-Longo PJ. Quantification of fibronectin matrix assembly sites using a novel ELISA assay. Matrix Biol 2007;26:330–333. [PubMed: 17257819]

Zheng M, McKeown-Longo PJ. Regulation of HEF1 expression and phosphorylation by TGF-β1 and cell adhesion. J Biol Chem 2002;277:39599–39608. [PubMed: 12189134]

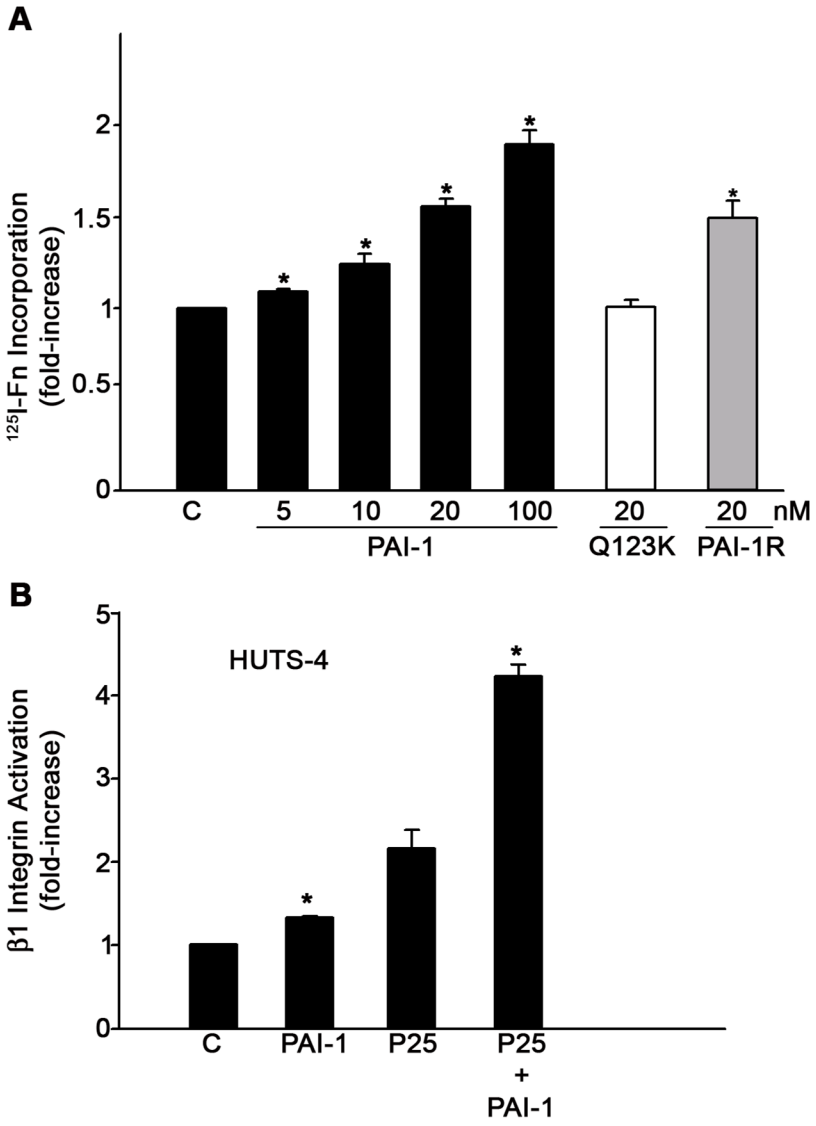

Fig. 1.

PAI-I increases fibronectin matrix assembly and β1 integrin activation in MG-63 cells. **A** - MG-63 cells were incubated with ^{125}I-fibronectin for 6 hours in the presence of the indicated concentrations of PAI-1, PAI-1R or PAI-1 (Q123K) in DMEM+BSA 0.02% + 20 mM Hepes. Cell layers were extracted with 1% DOC, and ^{125}I-fibronectin that was incorporated into the detergent-insoluble matrix was recovered by centrifugation and measured by gamma scintillation. This experiment is representative of three separate experiments. Data are the mean ± S.E. of two experiments performed in duplicate. *Significantly different than control cells, *t* test, $p < 0.05$ (n=4). **B** - MG-63 cells were pretreated with 20 nM PAI-1 for 20 minutes and incubated with 50 μM of uPAR agonist P25 or S25 for 1 hour in DMEM. Activation of β1 integrin was assessed by ELISA using the HUTS-4 antibody. Total β1 integrin was measured using the P5D2 antibody against α5β1. The graph shows the levels of β1 integrin activation after normalization to total β1 levels. Neither P25 nor PAI-1 had any effect on total β1 integrin. Data represent one of three different experiments performed in triplicate. *Significantly different than control or P25-treated cells, respectively, *t* test, $p < 0.05$ (n=3).

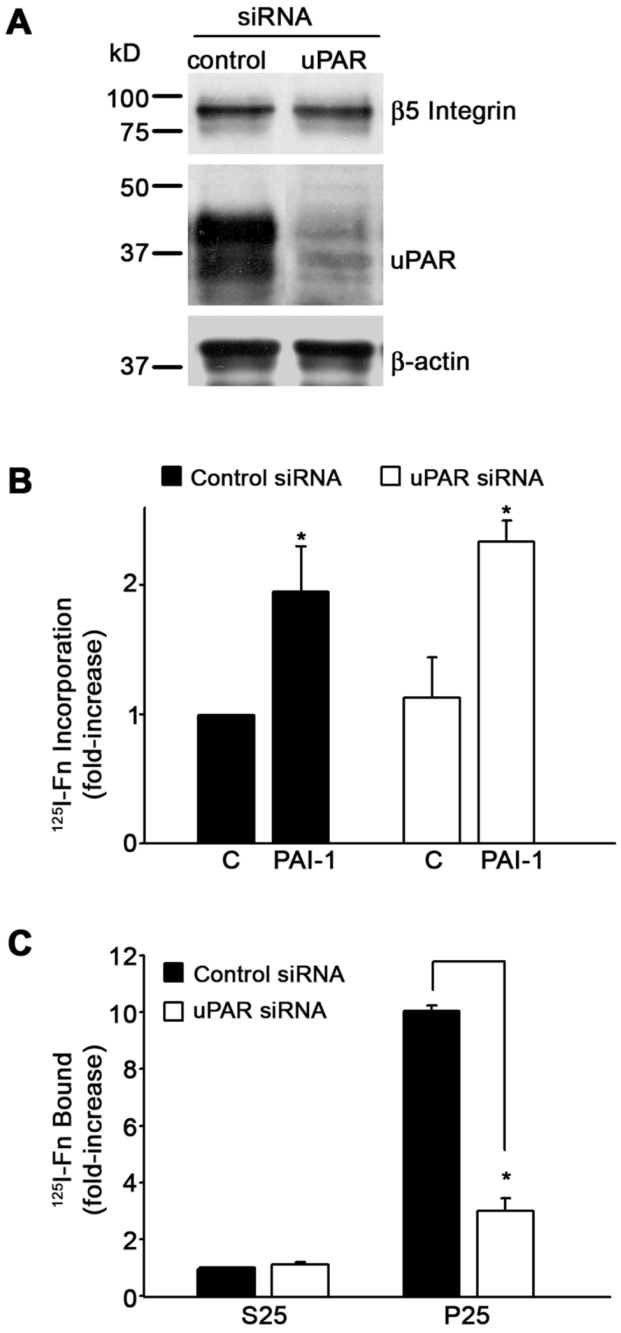

Fig. 2.

The PAI-1 mediated increase in fibronectin matrix assembly does not require uPAR. **A** - Cell lysates were prepared from control siRNA or uPAR siRNA transfected MG-63 cells. uPAR and β5 integrin levels were analyzed by Western blotting. The membrane was stripped and reprobed with anti β-actin antibody as a loading control. **B** - Cells layers from control siRNA or uPAR siRNA transfected MG-63 cells were incubated with ^{125}I-fibronectin for 6 hours in the absence or presence of PAI-1 (20 nM). Cell layers were extracted with 1% DOC, and ^{125}I-fibronectin that was incorporated into the detergent-insoluble matrix was recovered by centrifugation and measured by gamma scintillation. Data are the mean ± S.E. of two experiments performed in duplicate. *Significantly different than non treated cells, *t* test, $p <$

0.05 (n=4). **C** - Cells layers from control siRNA or uPAR siRNA transfected MG-63 cells were incubated with ^{125}I-fibronectin for 6 hours in the presence of the uPAR agonist P25 or the control peptide, S25. Cell layers were washed and scraped into 1% DOC and cell layer associated ^{125}I-fibronectin was measured by gamma scintillation. Data are the mean ± S.E. of two experiments performed in duplicate. *Significantly different than control cells, *t* test, $p < 0.05$ (n=4).

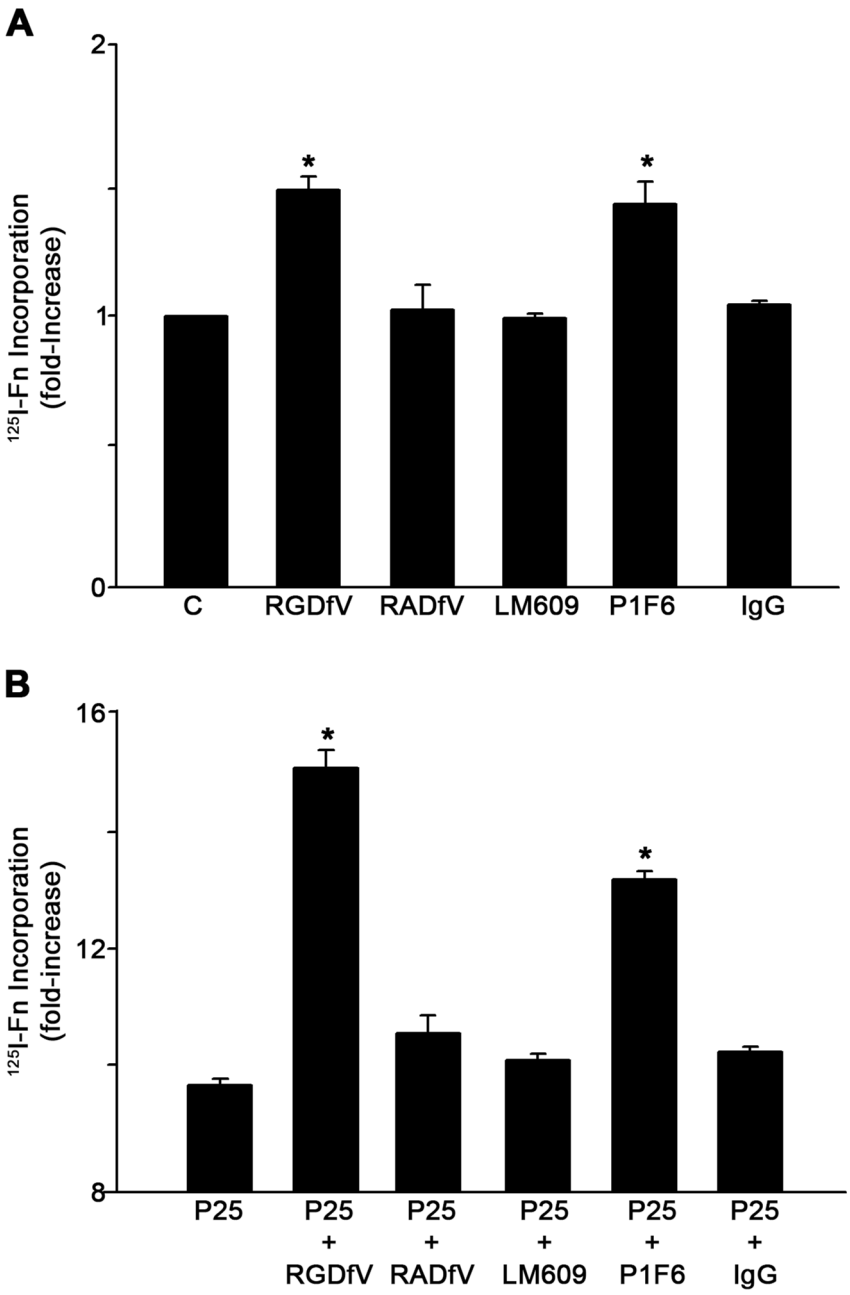

Fig. 3.

Inhibition of αvβ5 integrin interaction with vitronectin increases fibronectin matrix assembly. **A** - MG-63 cells were pre-incubated for 45 minutes with the cyclic peptide RGDfV (20 μM) or its inactive analog RADfV (20 μM) or for 2 hours with 20 μg/ml of normal mouse IgG, β3 integrin blocking antibody LM609 or β5 integrin blocking antibody P1F6 and then incubated with ^{125}I-fibronectin (Fn) for 6 hours. This experiment is representative of three separate experiments. Data are the mean ± S.E. of two different experiments performed in duplicate. *Significantly different than control cells, *t* test, $p < 0.05$ (n=4). **B** - Same as **A** only under conditions of uPAR stimulation with P25. Cell layers were extracted in 1% DOC, and ^{125}I-fibronectin that was incorporated into the detergent-insoluble matrix was recovered by centrifugation and measured by gamma scintillation.. This experiment is representative of three

separate experiments. Data are the mean ± S.E. of two experiments performed in duplicate. *Significantly different than P25-treated cells, *t* test, $p < 0.05$ (n=4).

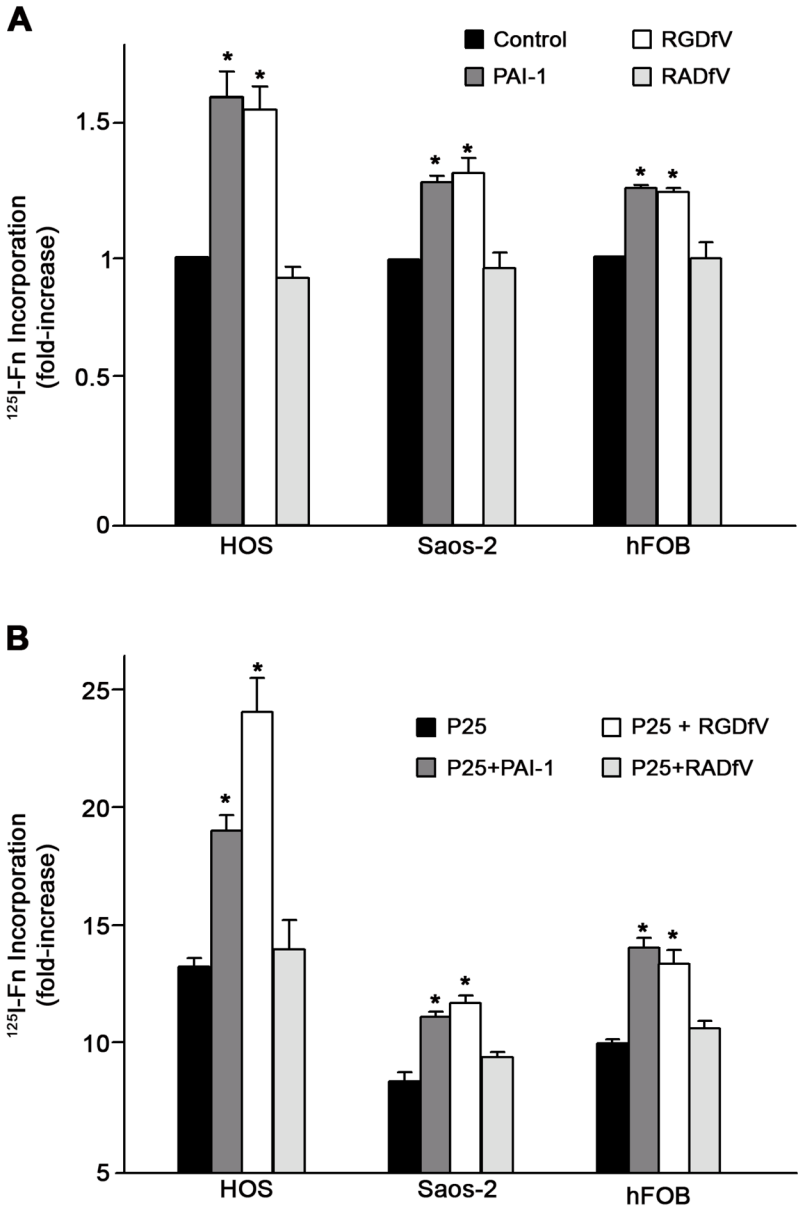

Fig. 4.

PAI-1 stimulates fibronectin matrix assembly in osteosarcoma and osteoblast cells. **A** - Cells were pre-incubated for 20 minutes with PAI-1 (20 nM) or for 45 minutes with the cyclic peptide RGDfV (20 μM) or its inactive analog RADfV (20 μM) and then incubated with ^{125}I-fibronectin (Fn) for 6 hours. Cell layers were extracted in 1% DOC, and ^{125}I-fibronectin that was incorporated into the detergent-insoluble matrix was recovered by centrifugation and measured by gamma scintillation. This experiment is representative of three separate experiments. Data are the mean ± S.E. of two different experiments performed in duplicate. *Significantly different than control cells, *t* test, $p < 0.05$ (n=4). **B** - Same as **A** only under conditions of uPAR stimulation with 50 μM P25. This experiment is representative of three separate experiments. Data are the mean ± S.E. of two experiments performed in duplicate. *Significantly different than P25-treated cells, *t* test, $p < 0.05$ (n=4).

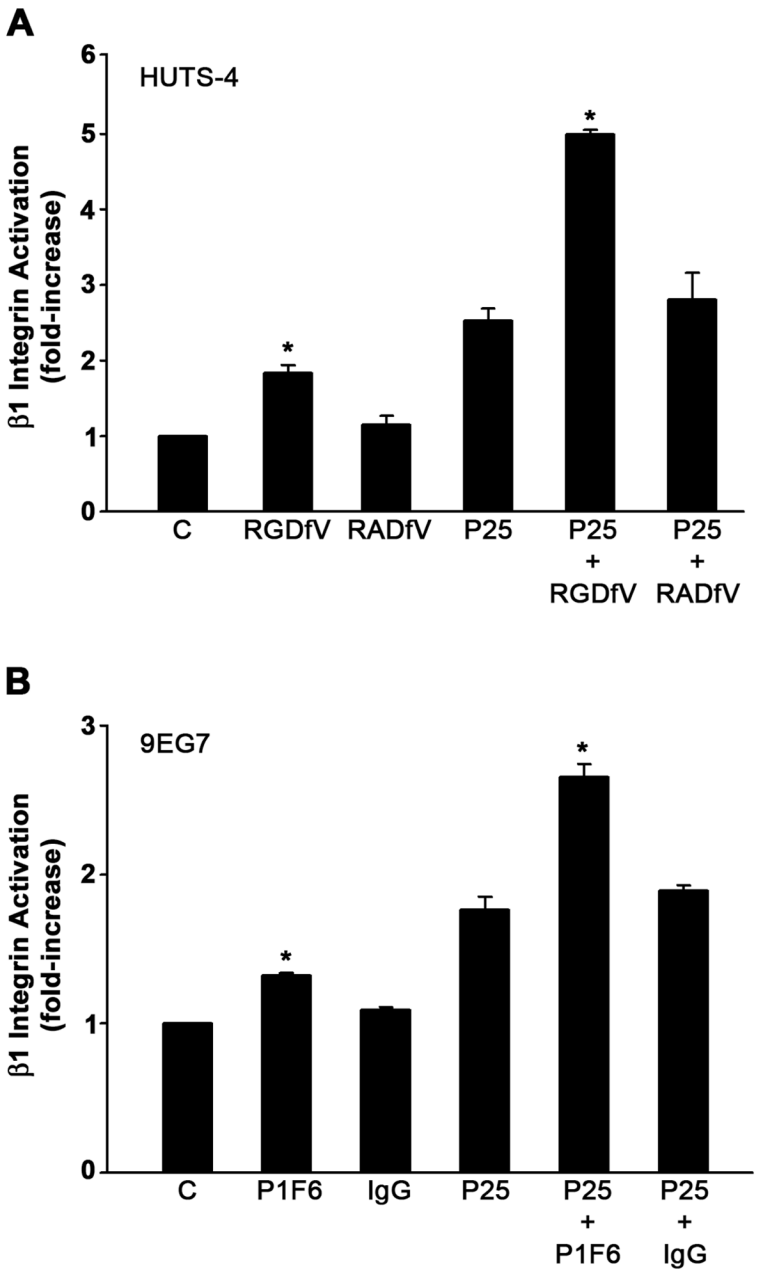

Fig. 5.

Activation of β1 integrin by β5 integrin blocking agents. **A** - MG-63 cells were pretreated for 45 minutes with 20 μM cyclic peptides RGDfV or RADfV and incubated with 50 μM of P25 or S25 in DMEM. Activation of β1 integrin was assessed by ELISA using the HUTS-4 antibody. B - MG-63 cells were preincubated for 2 hours with 20 μg/ml of normal mouse IgG, or β5 integrin blocking antibody P1F6 before treatment with P25 or S25. Integrin activation was assessed using monoclonal antibody 9EG7. All graphs show the levels of β1 integrin activation after normalization to total β1 levels as described in Fig. 1. Total β1 integrin did not change. Data represent one of three different experiments performed in triplicate. *Significantly different than control or P25-treated cells, respectively, *t* test, $p < 0.05$ (n=3).

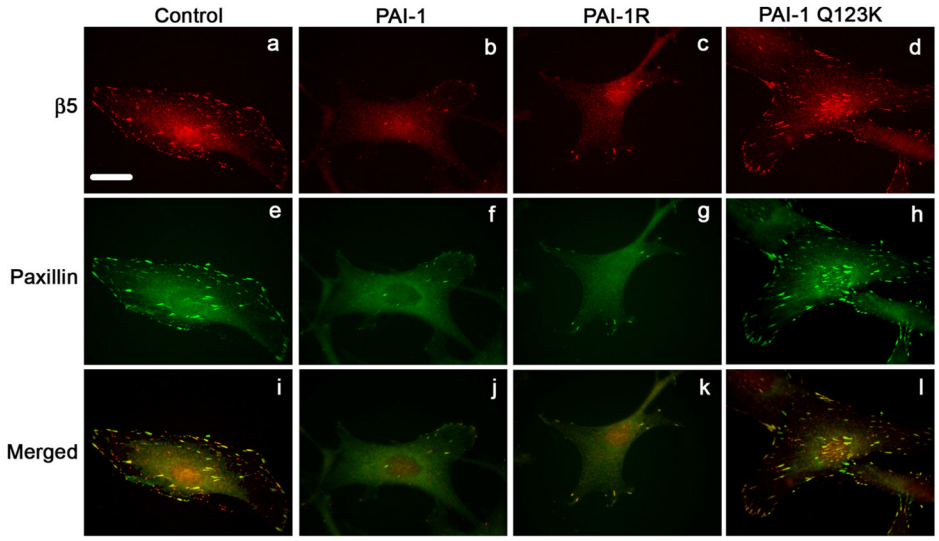

Fig. 6.

PAI-1 disrupts focal adhesions. MG-63 cell monolayers were plated overnight onto coverslips in complete media and then incubated for 3 hours with 20 nM of PAI-1 or PAI-1 mutants (PAI-1R and Q123K). Cells were subsequently fixed, permeabilized and stained for 1 hour with the clone 15F11 antibody for β5 integrin (panels a-d). After1 hour staining with the AlexaFluor^{594} derivatized anti-mouse secondary antibody, cells were washed and labeled for an additional hour with a paxillin-FITC antibody (panels e-h). Panels i-l show merged images indicating colocalization of β5 integrin with paxillin. Scale Bar, 20 μm.

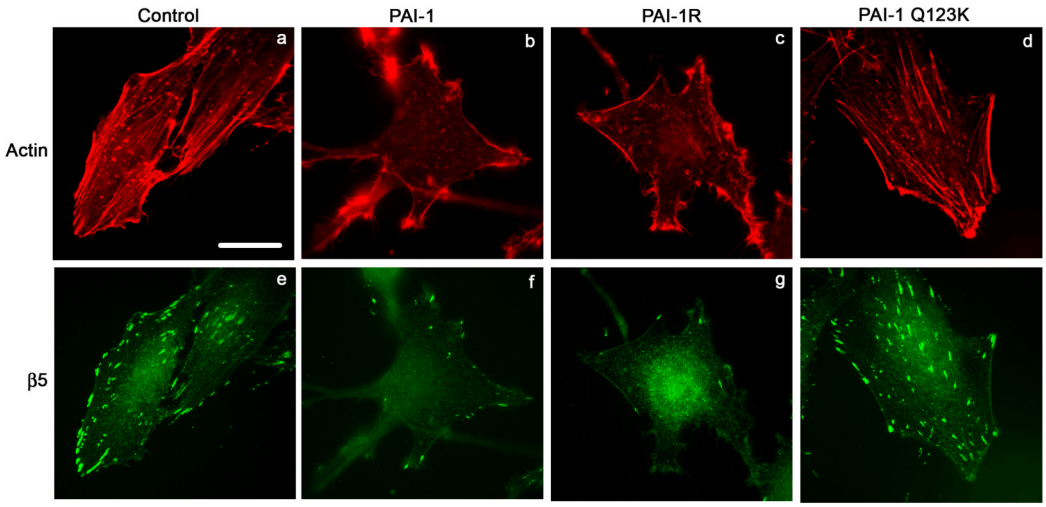

Fig. 7.

PAI-1 disrupts actin stress fibers. MG-63 cell monolayers were plated overnight onto coverslips in complete media and then incubated for 3 hours with 20 nM of PAI-1 or PAI-1 mutants (PAI-1R and Q123K). Cells were subsequently fixed, permeabilized and stained for 1 hour with the clone 15F11 antibody for β5 integrin. Cells were then washed and labeled for an additional hour with the AlexaFluor^{488} derivatized anti-mouse secondary antibody and the AlexaFluor^{594}-phalloidin. Actin and β5 integrin were visualized by indirect immunofluorescence. Scale Bar, 20 μm.

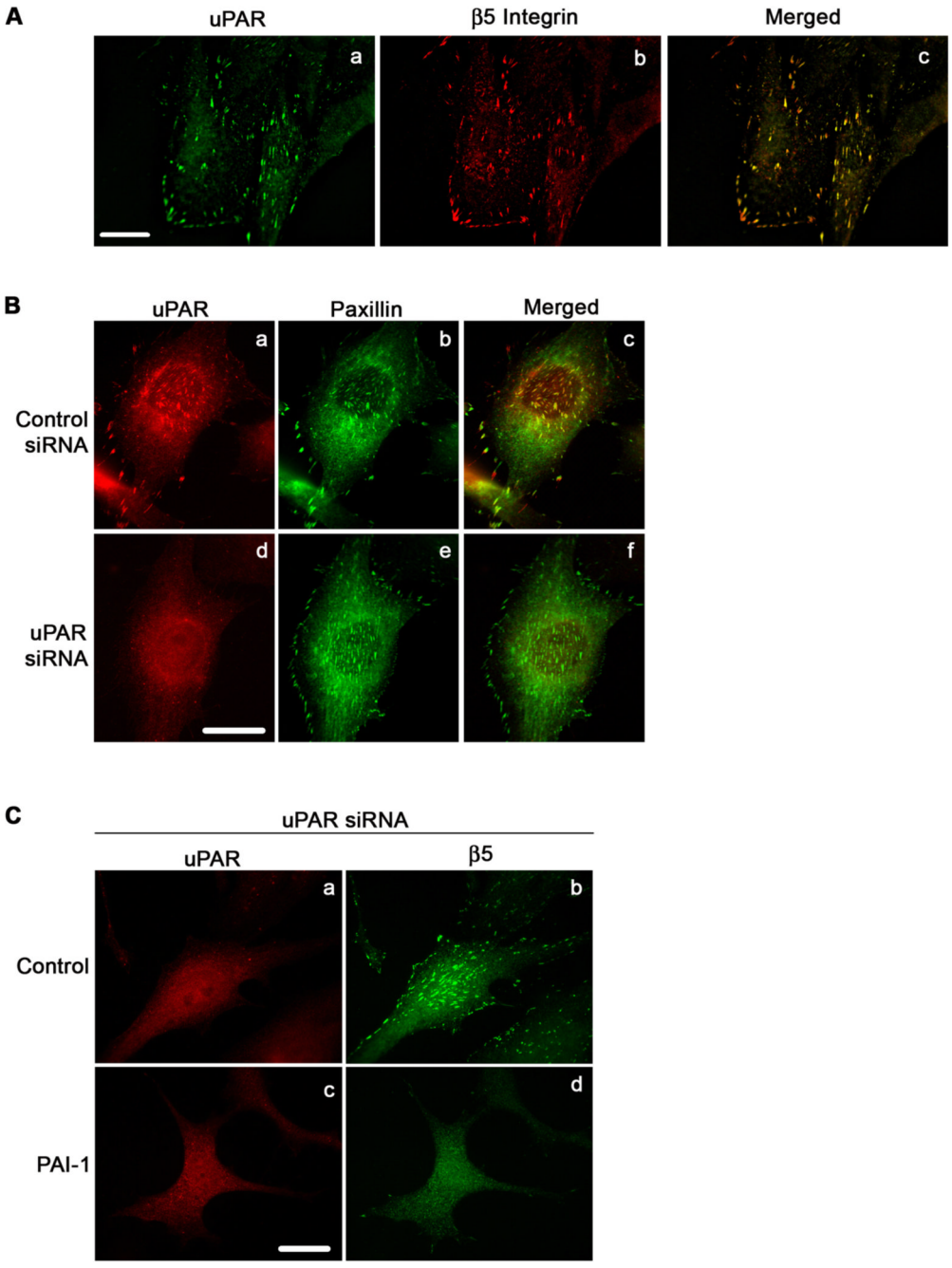

Fig. 8.

PAI-1 mediated disruption of focal adhesions does not require uPAR. **A** - MG-63 cells were plated overnight in complete medium. Cells were subsequently fixed, permeabilized and stained with uPAR polyclonal antibody (panel a) and 15F11 monoclonal antibody for β5 integrin (Panel b). uPAR and β5 integrin were visualized by indirect immunofluorescence. Panel c shows the merged image. Scale Bar, 20 μm. **B** - Cells stained for uPAR and paxillin. Panels a and b show uPAR and paxillin staining in control siRNA treated cells. Panels d and e show uPAR and paxillin staining in uPAR knock down cells. Panels c and f are the merged images. Yellow indicates colocalization of uPAR and α5 integrin. Scale Bar, 20 μm. **C** - uPAR siRNA treated cells were plated overnight in complete medium and then incubated for 3 hours

in DMEM in the presence or absence of PAI-1. Scale Bar, 20 μm. Cells were subsequently fixed, permeabilized and stained. uPAR and β5 integrin were visualized by indirect immuno-fluorescence in non-treated cells (panels a and b) and PAI-1 treated cells (panels c and d).

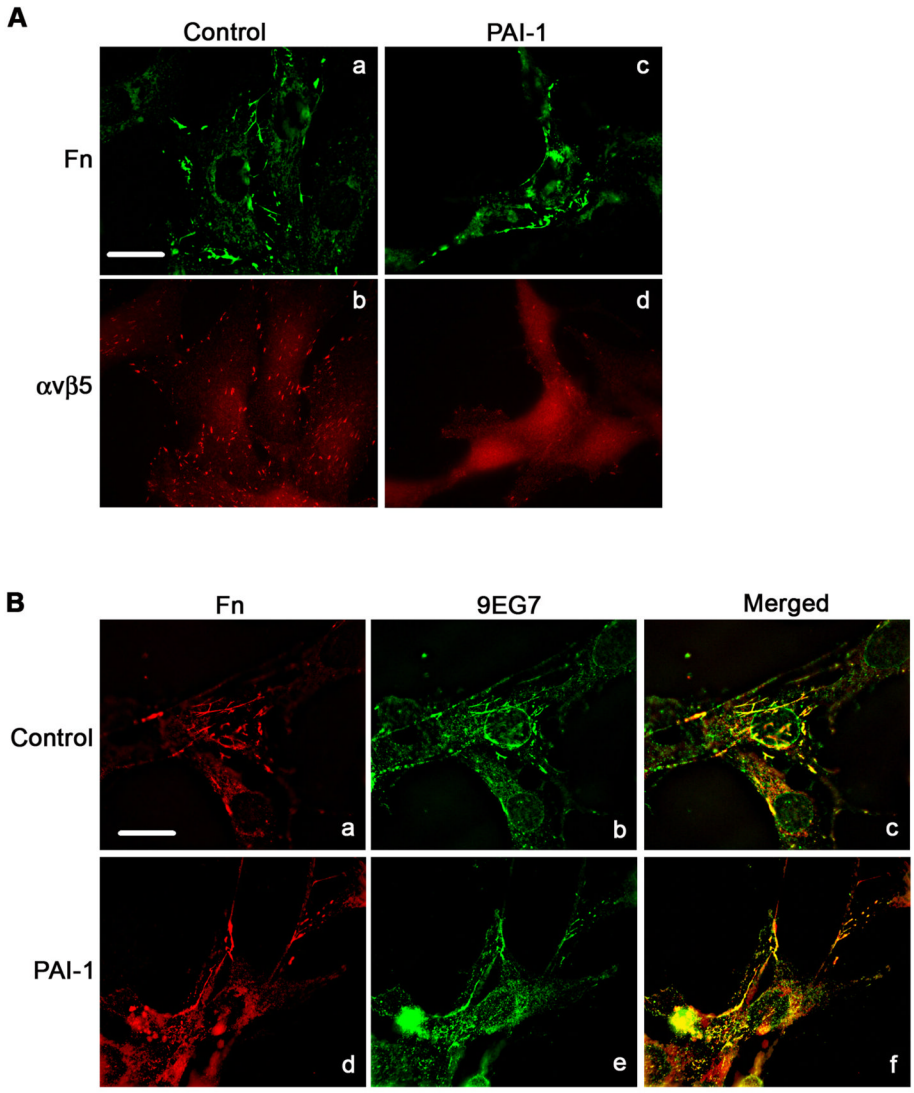

Fig. 9.

PAI-1 does not disrupt the association of α5β1 with fibronectin matrix. Cells were incubated for 3 hours in DMEM in the presence or absence of PAI-1, subsequently fixed, permeabilized and immunostained. **A** - Fibronectin matrix and β5 integrin were visualized by indirect immunofluorescence in non-treated cells (panels a and b) and PAI-1 treated cells (panels c and d). Scale Bar, 20 μm. **B** - Fibronectin and activated β1 integrin (detected with 9EG7 antibody) were visualized by indirect immunofluorescence in non-treated cells (panels a and b) and PAI-1 treated cells (panels d and e). Panels c and f shows merged pictures. Yellow staining indicates areas of colocalization of β1 integrin with fibronectin matrix. Scale Bar, 20 μm.

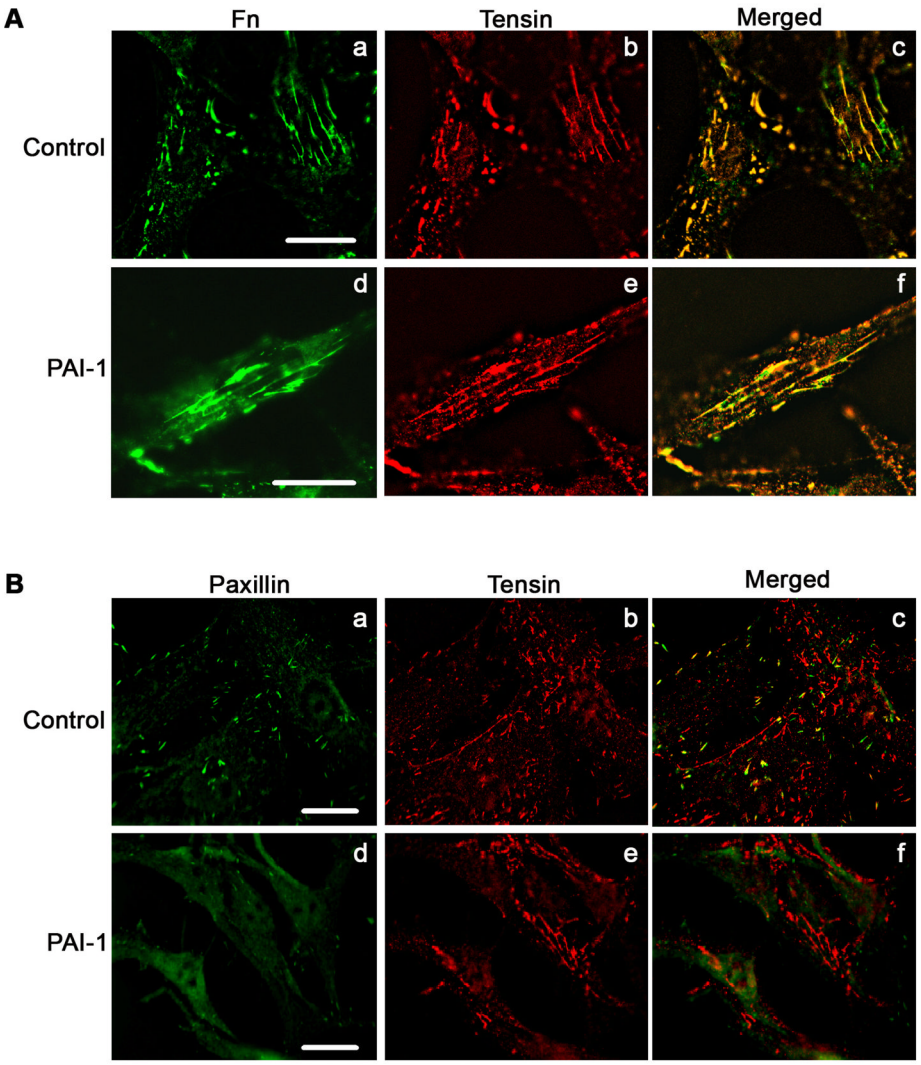

Fig. 10.

PAI-1 does not disrupt matrix adhesions. Cells were incubated overnight onto coverslips in complete media and then incubated for 3 hours in DMEM in the presence or absence of PAI-1 (20 nM). Cells were subsequently fixed, and permeabilized. A - Fibronectin and tensin were visualized by indirect immunofluorescence in non-treated cells (panels a and b) and PAI-1 treated cells (panels d and e). Panels c and e show the merged pictures. Yellow staining represents area of colocalization of tensin and fibronectin. Scale Bar, 20 μm. **B** – Paxillin and tensin were visualized by direct and indirect immunofluorescence in non-treated cells (panels a and b) and PAI-1 treated cells (panels d and e). Panels c and f shows merged pictures. Scale Bar, 20 μm.

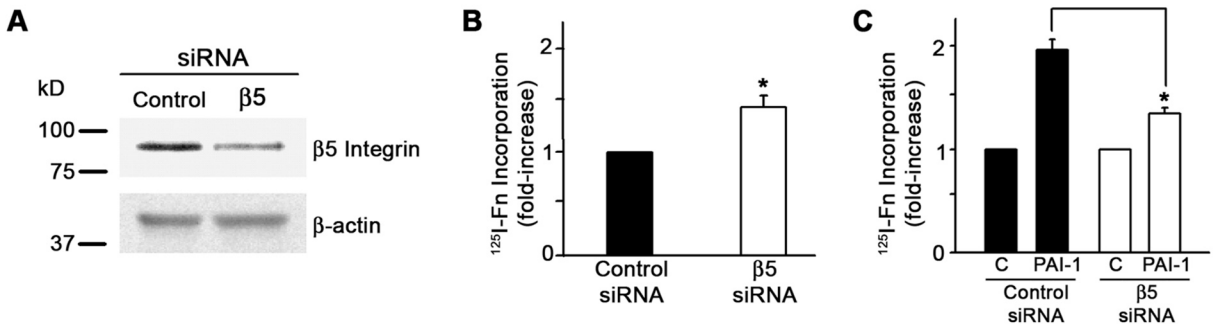

Fig. 11.

β5 knockdown inhibits PAI-1 stimulation of matrix assembly. **A -** Lysates from MG-63 cells treated with either control siRNA or β5 siRNA were analyzed for β5 integrin and actin by Western blot. **B, C -** MG-63 cells treated with either control or β5 siRNA were incubated with ^{125}I-fibronectin for 6 hours in the presence of 20 nM PAI. Cells were extracted with 1% DOC and ^{125}I-fibronectin incorporated into detergent insoluble matrix was recovered by centrifugation and measured by gamma scintillation. Experiments are representative of separate experiments performed in triplicate. Data are the mean ± S.E. of one experiment performed in triplicate. *t* test, $p<0.05$ (n=3). All values were normalized to protein content. No significant difference in protein content was observed between control siRNA and β5 siRNA treated cells.

Table 1

Number of Focal Contacts

	1–10	10–20	Over 20
No Treatment	-	-	100%
PAI-1	98%	2%	-
PAI-1R	94%	6%	-
Q123K	-	-	100%

To examine the number of focal contacts, MG-63 cells were plated overnight onto coverslips in complete medium, and incubated for 3 hours with 20 nM PAI-1 or PAI-1 mutants (PAI-1R and Q123K). Cells were fixed, permeabilized and stained for paxillin. Focal contacts were visualized using an Olympus BMX-60 microscope (100X). 200 cells were analyzed for each treatment. The % of cells containing the indicated number of focal contacts is shown.